Infrared Physics and Technology 99 (2019) 201–211

Contents lists available at ScienceDirect

Infrared Physics & Technology

journal homepage: www.elsevier.com/locate/infrared

Regular article

Evaluating the efficiency of infrared breast thermography for early breast cancer risk prediction in asymptomatic population

Usha Rani Gogoi[a], Gautam Majumdar[b,*], Mrinal Kanti Bhowmik[a], Anjan Kumar Ghosh[a]

[a] Department of Computer Science & Engineering, Tripura University, (A Central University), Suryamaninagar 799022, Tripura, India
[b] Department of Radiotherapy, Regional Cancer Centre, Agartala Govt. Medical College, Agartala 799006, Tripura, India

ARTICLE INFO

Keywords:
Breast cancer
Early breast abnormality prediction
Infrared breast thermography
Routine check-up tool
Asymptomatic Patients

ABSTRACT

The high incidence and mortality rate of breast cancer in India and the limitations of gold standard method X-ray mammography to be used as a screening and diagnostic modality in young women tempted us to evaluate the efficiency of highly sensitive and non-radiating Infrared Breast Thermography (IBT) in early breast abnormality detection. This study investigates the efficiency of IBT by doing Temperature based analysis (TBA), Intensity based analysis (IBA), and Tumor Location Matching (TLM). In TBA and IBA, several temperature and intensity features were extracted from each thermogram to characterize healthy, benign and malignant breast thermograms. In TLM, the locations of suspicious regions in thermograms were matched with the tumor locations in mammograms/Fine Needle Aspiration Cytology images to prove the efficiency of IBT. Thirteen different sets of features have been created from the extracted temperature and intensity features and their classification performances have been evaluated by using Support Vector Machine with Radial basis function kernel. Among all feature sets, the feature set comprising the statistically significant ($p < 0.05$) features provides the highest classification accuracy of 83.22% with sensitivity 85.56% and specificity 73.23%. Based on the results of this study, IBT is found to be potential enough to be used as a proactive technique for early breast abnormality detection in asymptomatic population and hence, capable of identifying the subjects that need urgent medical attention.

1. Introduction

Breast cancer is the most commonly diagnosed cancer in female accounting for about one-third of all female cancers [1]. Studies showed that compared to 10% survival chance for late detection, early detection leads to 85% survival chance [2]. Hence, early detection is the key factor for reducing the incidence and mortality rates of breast cancer. However, due to the radiation risks of the gold standard method X-ray mammography (MG), it is not recommended for young women of age below 40 years, nursing and pregnant women [3–5]. Moreover, it has been reported that only 0% and 1.9% diagnosis were possible under the age group of 20 years and 20–34 years respectively [6]. These poor diagnosis rates and the restrictions of MG to be used in women of young age group tempted us to evaluate the efficiency of portable, highly sensitive, noninvasive, non-radiating, passive, fast, painless and inexpensive [7–9] Infrared Breast Thermography (IBT) in early detection of breast abnormalities so that it can be used for women of younger age group. The key idea for which IBT is applicable in breast abnormality detection is that due to the increased blood flow, angiogenesis and higher chemical and blood vessel activities, the regional surface temperature around the precancerous or cancerous tumor get increased [10] and IBT, being a functional imaging modality is capable of detecting this minute temperature changes as an early sign of breast abnormality. Thus, one of the popular methods for abnormality detection from thermograms is to examine the presence of hyperthermia and hypervascularity patterns related to tumor growth [11]. Due to its capability of detecting any raise in temperature, IBT can detect the first sign of developing a cancer tumor 8–10 years before MG can detect it [12,13].

Based on an IBT based study, Gamagami [14] reported that IBT was capable of detecting cancers in 15% cases, which were not discernible by MG. They also concluded that in 86% of non-palpable breast cancer cases, the hypervascularity and hyperthermia were visible [14]. In literature several studies have been made on temperature based analysis of breast thermograms. In [15], Sarigoz et al. by doing a temperature based analysis concluded that IBT can differentiate the benign lesions from malignant lesions with sensitivity up to 95.24% and specificity up to 72.73%. Louis [16] confirmed that the abnormal patterns in the

* Corresponding author.
E-mail address: gmagmc18@gmail.com (G. Majumdar).

https://doi.org/10.1016/j.infrared.2019.01.004
Received 7 September 2018; Received in revised form 3 January 2019; Accepted 3 January 2019
Available online 04 January 2019
1350-4495/

infrared images are the highest risk indicators of breast cancer development in future. Based on a numerical study, Ng and Fork [17] concluded that the average mean temperature of breast for healthy patients is 32.66 °C and for benign patients is 32.81 °C and for carcinoma patients is 33.43 °C. In brief Ng and Fork's investigations showed that carcinoma patients generally have higher breast temperature compared to those of healthy patients and even benign patients. Although these studies evaluated the potentiality of IBT in early breast abnormality detection through temperature based analysis, the potentiality of IBT in locating the suspicious regions is still not investigating in any of the existing research works. So, in this study our objective is to first validate the findings of IBT with the clinical findings, mammography and Fine Needle Aspiration Cytology (FNAC) reports and then, evaluate the efficiency and potentiality of IBT in early breast abnormality predictions. Doing so, one can use IBT as a routine checkup tool in asymptomatic population and thus, identify the patients that need urgent medical attention. The key contributions of this study are as follows-

(a) The potentiality of Temperature Based Analysis (TBA) for discriminating the healthy thermograms from the benign and malignant ones has been investigated.
(b) The discriminability of Intensity Based Analysis (IBA) of breast thermograms in differentiating healthy, benign and malignant thermograms has been evaluated.
(c) The performance of each combination of TBA and IBA features has been evaluated to obtain the most optimal feature set that gives the highest classification accuracy.
(d) The locations of suspicious regions in breast thermograms are matched with the tumor locations in mammograms.

The rest of the paper is organized as follows. The designing of a standard breast thermogram acquisition protocol along with the establishment of a breast thermogram acquisition setup has been described in Section 2. The validation of the collected breast thermograms has also been done in Section 2. Section 3 describes the analysis of breast thermograms. Section 4 demonstrates the experimental results. Finally, Section 5 and 6 discuss and conclude the paper respectively.

2. Materials

2.1. Acquisition of Infrared Breast Thermograms

In order to evaluate the efficiency of IBT in early breast abnormality detection, the development of a real-time breast thermogram database is very crucial. However, the accuracy of IBT relies on several factors and neglecting these factors may hamper and degrade the efficiency and sensitivity of IBT. In [18], Ring et al. had stated that IBT can produce a consistent result if certain standards are followed during thermography. Hence, the acquisition of breast thermograms should be performed under some strict protocols.

2.1.1. Designing of a standard acquisition protocol suite

Considering the necessity of designing a breast thermogram acquisition protocol, an IBT setup along with a standard acquisition protocol suite has been designed. Our proposed standard IBT acquisition procedure comprises of several necessary components including patient preparation, patient acclimation, environment of the examination room, the thermal imager system, patient positioning and capturing views. Each of these components has its influence on the efficiency of IBT. Hence, the standardization of IBT should maintain all these factors. The breast thermogram acquisition setup has been established at Regional Cancer Centre (RCC), Agartala Govt. Medical College, Tripura, India. A brief overview of each factor of acquisition protocol is provided in Table 1. The detailed description of each of these factors is provided in our previous work [19,20].

2.1.2. Statistics of the collected breast thermograms

This study is conducted on a breast thermogram dataset of 60 female subjects including 25 healthy, 23 benign and 12 malignant cases and this study is approved by a human subjects committee. Data are then analyzed for clinico-demographic information such as age, tobacco, or alcohol consumption, consumption of oral contraceptives, number of children, time of menarche, family history of any type of cancer etc. Table 2 demonstrates the patient characteristics of collected thermograms of each group.

Healthy Group: As illustrated in Table 2, the majority of healthy females (68%) included in this study are in the age group of 40–60 years. The mean age of the females is 48 ± 12 years. The tobacco consumption is found in almost 44% females. Around 60% of females are having their menarche at the age of 12 years or less, while remaining 40% have their menarche at the age of 13 years or more. Out of all healthy females, 48% are having their marriage before 18 years of age. Around 48% females are having 1 or 2 children and 44% are having 3 or more children. The intake of oral contraceptive is found in only 20% females and 16% of females have the family history of having cancer.

Benign Group: As illustrated in Table 2, around 87% benign females are of age 60 years or less. The mean age of the group is 42 ± 13 years. About 35% of females consume tobacco and 96% of females get their menarche at the age of 12 years or more. Majority of females (61%) are having their marriage at the age of 18 years or more and 83% of females are found to have either 1 or 2 children. Only 22% of females are found to intake oral contraceptives and 13% of females have the family history of having cancer.

Malignant Group: Like the benign group, majority of females (92%) in malignant group also are of age 60 years or less. The mean age of the group is 49 ± 9 years. Only 25% females are found to have tobacco consumption and 92% of females get their menarche at the age of 12 years or more. Out of all malignant females, 58% are having their marriage at the age of 18 years or more. 50% of malignant females have 1 or 2 children and the remaining 50% have 3 or more children. The intake of oral contraceptive is found in 50% malignant females and 25% of females have the family history of having cancer.

2.1.3. Validation and Categorization of Infrared Breast Thermograms

To evaluate the efficiency of IBT in early breast abnormality detection, the validation of the findings of IBT with the findings of the gold standard methods is very crucial. Therefore, along with the thermograms we have also collected the clinical examination, MG and the FNAC reports (if available) of each subject undergoing IBT. A comparison of the outcome of the MG and FNAC reports with the findings of IBT has been illustrated in Table 3. Table 3 also depicts the findings of the clinical examination of each patient. Although, a collection of more than 100 breast thermograms has been made, but to prove the efficiency of IBT, we consider the thermograms of only those subjects which are found to be either healthy or unhealthy based on the results of either mammography or FNAC. As illustrated in Table 3, it has been seen that for each abnormal cases either benign or malignant, IBT is capable of identifying the abnormality by showing either an asymmetric thermal pattern or a higher temperature region. However, in three cases with Patient Id 29, 30 and 31 of the abnormal group in Table 3, IBT shows the presence of asymmetry and hotspots in thermograms even when their MG reports are normal. But, the presence of ultrasound-guided FNAC reports of these cases supports the findings of IBT and it confirms that IBT is also capable of showing the abnormalities which are not detectable (false negative) through the gold standard method MG. Similarly, for MG or FNAC result based healthy cases, IBT is also capable of showing the presence of symmetry between the two breasts. Thus, by validating the outcomes of IBT with the reports of MG/FNAC, we can conclude that it is possible to use IBT either as a safe routine check-up or adjunctive tool in both symptomatic and asymptomatic population to identify the cases that require urgent medical

Table 1
Different Factors of Breast Thermogram Acquisition Protocol.

Factors	Description
Patient preparation	The patients are instructed to avoid prolonged sun exposure, the application of lotion or ointment on breasts, physical activity, pain medication, smoking or consumption of alcohol on the day of breast thermography. Moreover, the patient is also instructed to come in her 5th − 12th day and 21st day of the menstrual cycle.
Patient intake form	Upon arrival on the day of examination, the patients are instructed to fill an *Intake Form* by giving her all personal information including name, age, sex, height, weight, etc. and disease related information like symptoms (if any), duration, etc.. The patient also provides her family history of breast cancer or any other cancer, previous medical tests, diagnoses, surgeries, physical therapies (if any), etc. The patients are also asked to give their written consent on the intake form for using their breast thermograms for the research purpose.
Patient acclimation	After taking the consent, the patient is brought to a private place inside the examination room and she is instructed to disrobe from her waist up and to remove jewelry like neckpieces, chain, etc. (if any). Then the patient is asked to lie down on a bed cum table for 15 min by keeping his/her hands over head.
Examination room, environmental condition	The size of the room is adequate to maintain a consistent temperature. The examination room is free from ventilators and windows. An air conditioner is placed in the room to maintain the room temperature in the range of 20–24 °C. For accurately monitoring the humidity of the examination room, a Thermo-Hygrometer has also been utilized. In the examination room, instead of incandescent light, fluorescent lighting is used.
Breast Thermogram Acquisition Setup	The breast thermogram acquisition setup comprises of 3 components: (a) An Infrared Camera: FLIR T650sc thermal camera with thermal sensitivity of $<$ 20 mK @ 30 °C, spectral range of 7.5–14.0 μm and image resolution of 640 × 480 pixels has been used for acquisition of breast thermograms. For mounting the thermal camera, a vertical height adjustable tripod stand with a heavy base is used. (b) A Black Cubicle: To have a homogeneous black background while capturing, a cubicle with black background has been used. This cubicle with the black background is also used for providing privacy to the patients during acclimation time. (c) A Bed cum Table: To perform the patient acclimation in lying position and to have different views of breast thermograms, a bed cum table has been designed.
Patient positioning	An alignment of about 90° is maintained in between the camera lens, and breast area of each patient. To improve the precision of the temperature readings and the interpretation accuracy of the thermograms, a distance of 1 m is kept between the thermal camera and the patient body.
Breast Thermogram Views	The capturing starts with the supine view of the breast, which is followed by the capturing of frontal view, left lateral view, right lateral view, left oblique view, right oblique view, and close up views of each breast.

Table 2
Patient characteristics.

Patient Parameters	Healthy (25)	Benign (23)	Malignant (12)
Age: $<$ 40	5	11	3
40–60	17	9	8
$>$ 60	3	3	1
Tobacco consumption	11	8	3
Menarche Age:			
$<$ 12	4	1	1
At 12	11	13	4
$>$ 12	10	9	7
Age at Marriage:			
$<$ 18 years	12	9	5
$>$ = 18 years	13	14	7
Number of Children:			
1–2	12	19	6
3–5	11	3	6
Intake of oral contraceptives	5	5	6
Family History of Breast cancer	4	3	3

attention and further evaluation. Based on the MG and FNAC reports, the experimental breast thermograms are categorized into three groups namely: Healthy, Benign and Malignant.

3. Method: Analysis of breast thermograms

This section evaluates the efficiency of IBT quantitatively. For quantitative representation of the findings of IBT, we adopt the method of temperature based analysis (TBA) and intensity based analysis (IBA) of the temperature and intensity matrix of thermograms respectively. The temperature matrix of each thermogram is extracted by using the FLIR Software tool and stored in the form of '.CSV' (Comma Separated Values) files. Meanwhile, it is worth mentioning that while doing the TBA and IBA of thermograms, it is necessary to discard the non-breast regions from breast thermograms before computing the temperature or intensity features. Hence prior to the TBA and IBA, the breast thermograms are manually cropped to discard the irrelevant regions like neck portion, area underneath the breast etc. and then the breast region was extracted out by using a semi-automatic segmentation method [21,22], where a breast mask of each cropped breast thermogram is created by manually selecting the lower breast boundary points. Now, for performing the TBA and IBA, it is necessary to extract the bilateral temperature and intensity values from a breast thermogram. Fig. 1 depicts the procedure of extracting the bilateral temperature values from a breast thermogram which involves the following steps.

Step1: Obtain the cropped temperature matrix of the cropped breast thermogram.
Step2: Convolve the cropped temperature matrix with the corresponding breast mask.
Step3: Extract the temperature values inherent to breast region only.
Step4: Separate the temperature values of left and right breast.

In IBA, the same procedure is used to extract the bilateral intensity values from each breast thermogram. Fig. 2 depicts the segmented breast regions of some sample breast thermograms. Along with the TBA and IBA, a tumor location matching (TLM) analysis has also been performed, where the locations of suspicious regions in thermograms are matched with the tumor locations in mammograms/FNAC images. The details of each of these TBA, IBA and TLM are provided below.

3.1. Temperature Based Analysis (TBA) of thermograms

Since 400 BCE, the temperature has been used for clinical diagnosis [13,23]. Being homeothermic, the human is capable of maintaining a constant temperature in the body and to have the normal performance of the human body, it is essential to regulate the inner core temperature. A small change of core temperature is a clear indication of probable illness [24]. Hardy [25,26] established the diagnostic importance of temperature measurement by infrared technique, which introduced the concept of using infrared thermography in medical science. In 1963, Barnes demonstrated that thermograms can provide information of physiological anomalies and hence, useful for diagnosis of physical illness [27].

TBA investigates the capability of thermal patterns in discriminating

Table 3
Medical Information of all Patients with and without Abnormal Findings.

Patient Id.	Age (yrs.)	Self-Examination/Duration	Clinical Observation	Mammo Report	Location based on Mammo	FNAC/ Biopsy	Thermogram Result
			ABNORMAL SUBJECTS				
1	36	Pain, Discharge, Lump (Lt)/11 months	Not Provided	FA (Lt)	UOQ	–	Asym
2	55	Lump (Lt)/6–7 months	Lump (Lt)	MT (Lt)	LIQ	MT (Lt)	HS (Lt), Asym
3	62	Pain, Tenderness, Discharge, Lump (Lt)/6 months	Lump (Lt)	MT (Lt)	UOQ	–	HS (Lt), Asym
4	27	Pain, Lump (Lt)/1 month	Not Provided	FL (Lt)	UOQ	–	Asym
5	56	Pain, lump (Lt), skin is reddish/6 months	Lump (Lt)	MT (Lt)	UA	DC (Lt)	HS (Lt), Asym
6	46	Pain, Heaviness, Lump (Lt)/1 year	Lump (Lt)	MT (Lt)	PA	MT (Lt)	HS (Lt), Asym
7	58	Pain, Tenderness, Lump (Lt)/3 months,	Lump (Lt)	MT (Lt)	UOQ	MT (Lt)	Asym
8	41	Pain, Lump (Lt)/2 months	Nodular Fasciitis (Lt)	BT (Lt)	LIQ	–	Asym
9	39	Pain , Tenderness , Lump (Lt)/2 month,	Lump (Lt)	MT (Lt)	UOQ	DC (Lt)	HS (Lt), Asym
10	41	Pain, Tenderness, lump (both)/5 years,	Not Provided	DE (Both)	UIQ	–	Sym
11	28	Tenderness, Lump (Rt)/2 month	Swelling (Rt)	BT (Rt)	UOQ	BT (Rt)	HS (Rt), Asym
12	60	Pain (Lt)/ 1 month/Breast Cancer (Lt) 8 years back	Lump (Lt)	FL (Lt)	UIQ	–	Asym
13	25	Pain, Tenderness, Lump, discharge (both)/5 years	FD (Both)	FD (Both)	UOQ	–	HS (Rt), Asym
14	54	Pain, Tenderness, Lump (Rt)/4 month	Lump (Rt)	MT (Rt)	UOQ	MT (Rt)	HS (Rt), Asym
15	35	Pain, Lump (Lt), Inverted nipple (Lt), Heavy milky discharge (Lt)/2 weeks	Fibroadenosis (Left)	MT (Lt)	UOQ	–	HS (Lt), Asym
16	30	Pain (Both), Tenderness, Lump (Rt)/2 years	Fibroadenosis (Both)	FD (Both)	–	–	HS (Both), Asym
17	38	Lump (Rt)/1 month	Lump (Rt)	MT (Rt)	PA	DC (Rt)	HS (Rt), Asym
18	47	Pain, Tenderness, Lump (Both), milky discharge (both)/9 years	Lump (Both)	BT (Both)	–	–	HS (Both)
19	40	Pain, Tenderness, Lump (Rt), swelling of right hand, Inverted nipple (Rt) /1 year	Lump (Rt)	MT (Rt)	UIQ	DC (Rt)	HS (Rt), Asym
20	30	Pain, Lumps, yellowish discharge (left)/3 months	Not Provided	BT (Lt)	–	IG (Lt)	HS (Lt), Asym
21	21	Pain, Tenderness, Lumps(both)/4 months	Lump (Both)	BT (Rt)	–	FA (Both)	HS (Both)
22	70	Pain, Lump (Rt)/1 month	Lump (Rt)	Cal (Rt)	–	–	HS (Rt), Asym
23	40	Tenderness, Lumps (Rt)/2 years	Lump (Rt)	BT (Rt)	UIQ	BT (Rt)	HS (Rt), Asym
24	47	Pain, Lump (Lt)/3–4 weeks	Lump (Both)	FA (Lt)	–	–	HS (Both), Asym
25	65	Pain, Heaviness, lump (Lt)/6 months	Lump (Lt)	BT (Lt)	–	–	HS (Lt), Asym
26	35	Lump, yellowish discharge (Lt)/6 months	Lump (Lt)	BT (Lt)	UIQ	FA (Lt)	HS (Lt), Asym
27	60	Pinprick pain, Lump (Lt)/3 weeks	Lump (Lt)	MT (Lt)	UIQ	MT (Lt)	HS (Lt , Asym
28	32	Pain, Lumps (Both)/7 years	Lump (Rt)	BT (Rt)	UIQ	–	HS (Both), Asym
29	49	Pain, Lump (Lt), skin is reddish/2 week	Lump (Lt)	DB	PA	BT (Lt)	HS (Lt), Asym
30	47	Pain, Burning, Lump (Lt)/2 months	Swelling (Lt)	N	UIQ	DC (Lt)	HS (Lt), Asym
31	36	Lump (Rt)/3 months	Fibrocystic (Rt)	N	–	BT (Rt)	Asm
32	61	Skin is Reddish (Rt)	Skin Ulcer (Rt)	DB	–	Ulcer (Rt)	HS (Lt), Asym
33	37	Pain (Lt) /3 months/FD (Rt) 2 years back	Fibroadenosis (Rt)	FA (Lt)	–	–	HS (Lt), Asym
34	35	Pin prick pain (Both)/1 year	Swelling (Both)	BT (Both)	–	–	Asym
35	60	Pain, Heavy PUS Formation(Lt)/2 weeks	Abscess, Swelling (Lt)	FA (Lt)	–	–	HS (Lt), Asym
			NORMAL SUBJECTS				
1	43	No symptom (Just Screening)	Not Provided	N	–	NA	Symmetric
2	46	Pain, Tenderness (B/L)/2 yrs.	Not Provided	N	–	NA	Symmetric
3	27	Pain (Rt)/1 yrs.	Not Provided	N	–	NA	Symmetric
4	40	Pain, Tenderness (Rt), Lump (Rt)/5 months	Lumpiness (Rt)	N	–	NA	Mild Asym
5	68	Pain, Lump (Rt)/3 months,	Not Provided	N	–	NA	Symmetric
6	49	Pain, Tenderness, Lump (Lt)/3 months	Not Provided	N	–	NA	Symmetric
7	58	Pain, Tenderness, Lump (Rt)/1 month	Not Provided	N	–	NA	Symmetric
8	60	Pain, Tenderness, Lump (Rt)/1 yr.	Lump (Rt)	N	–	NA	Symmetric
9	39	Burning Sensation (Rt)/2 months	Swelling (Rt)	N	–	NA	Symmetric
10	38	Pain, Lump (B/L)/3 months	Not Provided	N	–	NA	Symmetric
11	36	Lump (Rt)/1 week	Not Provided	N	–	NA	Symmetric
12	40	Pain, Tenderness, Lump (B/L)/3 months	Not Provided	N	–	NA	Symmetric
13	35	Pain (Rt)/1 + yrs., Lump (Rt)/1 week	Not Provided	N	–	NA	Symmetric
14	46	Lump (B/L), Milky discharge (B/L)/long time	Discharge (B/L)	N	–	NA	Symmetric
15	70	Pain, Lump (Lt)/1 yr.	Not Provided	N	–	NA	Symmetric
16	42	Pain (Rt), White liquid discharge (B/L)/1 week	Discharge (B/L)	N	–	NA	Symmetric
17	40	Pain, Lump (Rt)/2 months	Lump (Rt)	N	–	NA	Mild Asym
18	47	Pain, Lump, Milky discharge (B/L)/9 yrs.	Discharge (B/L)	N	–	NA	Symmetric
19	45	Pain, Tenderness (Lt), Discharge (Lt)/1 month	Discharge (Lt)	N	–	NA	Symmetric
20	45	Pain (Rt)/1 week, Tenderness (Rt)/5 months	Not Provided	N	–	NA	Symmetric
21	45	Tenderness, Lump (B/L)/2 months	Not Provided	N	–	NA	Symmetric
22	52	Pain, Tenderness (Rt)/2 weeks, Severe Back pain	Not Provided	N	–	NA	Symmetric
23	70	Pain, Lump (Lt)/1 yr.	Not Provided	N	–	NA	Symmetric
24	50	Pain (B/L)/10 yrs.	Mastalgia	N	–	NA	Symmetric
25	53	Pain, Lump (Lt)/2yrs	Lump (Lt)	DB	–	NA	Symmetric

Rt – Right, Lt – Left, Asym – Asymmetric, Sym – Symmetric, HS – Hotspot, MT – Malignant Tumor, BT – Benign Tumor, DC - Ductal Carcinoma, FA – Fibroadenoma, MC - Mucinous Carcinoma, DE - Ductal Ectasia, F – Fibroids, FD – Fibroadenosis, Cal - Vascular Calcification, FL – Focal Lesion, IG – Infected Galactocele, FC – Fibrocystic Disease, UOQ - Upper Outer Quadrant, LIQ - Lower Inner quadrant, UIQ - Upper Inner quadrant, LOQ - lower outer quadrant, UA – Under Arm, PA – Periareolar, N – Normal Study, DB – Dense Breast.

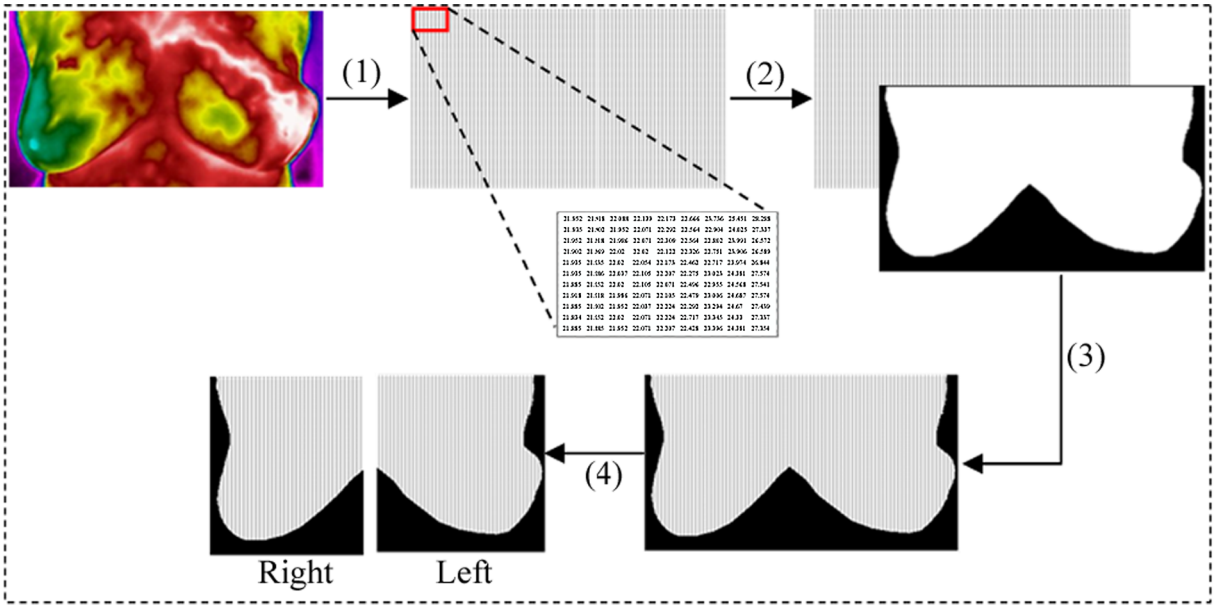

Fig. 1. Extraction of bilateral temperature values of a breast thermogram.

healthy, benign and malignant breast thermograms. To quantitatively represent the thermal patterns, four different temperature features namely mean, maximum, mode [28,29] and median temperature have been extracted from both left and right breasts. Extraction of these temperature features is followed by the computation of the temperature difference between both breasts of a thermogram. Based on the property of abnormal thermograms of having a significant temperature difference between two breasts, we have tested the statistical significance of the temperature analysis in breast abnormality detection. The statistical significance of the temperature features in discriminating between (a) healthy and benign, (b) healthy and malignant and (c) benign and malignant have been measured. For the statistical test, the Wilcoxon non-parametric test with significance level of 5% has been used. The average of the temperature differences of all breast thermograms of the benign, malignant and healthy groups along with their statistical significance values (p-value) are tabulated in Table 4.

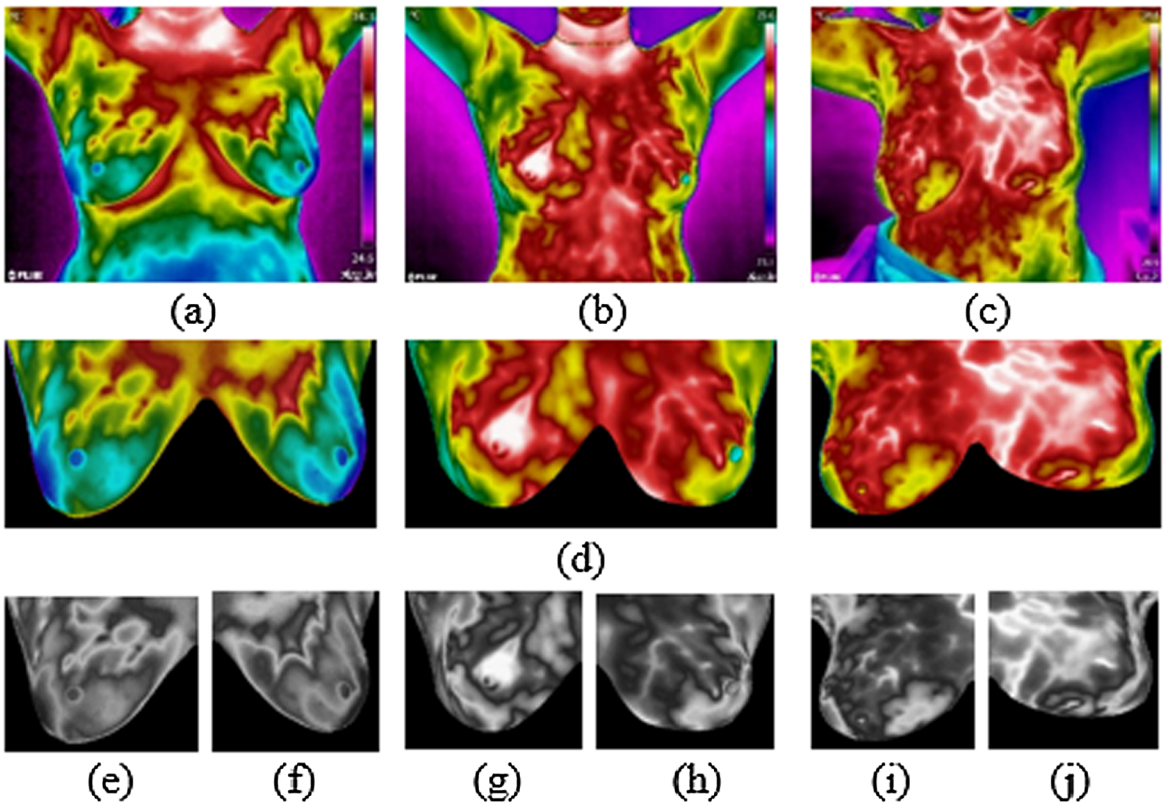

Fig. 2. (a) Healthy breast thermogram, (b) Benign breast thermogram, (c) Malignant breast thermogram, (d) Segmented breast regions of corresponding breast thermograms, (e, g, i) Right breasts and (f, h, j) Left breasts of corresponding breast thermograms.

Table 4
Bilateral temperature difference in each category of breast thermograms.

Temperature features	Healthy (H)	Benign (B)	Malignant (M)	p-val (H Vs. B)	p-val (H Vs. M)	p-val (B Vs. M)
Mean	0.309 ± 0.242	0.625 ± 0.612	1.000 ± 0.607	**0.0345 < 0.05**	**0.00002 < 0.05**	**0.0156 < 0.05**
Maximum	0.455 ± 0.446	0.682 ± 0.582	1.197 ± 1.016	0.1118 > 0.05	**0.0121 < 0.05**	0.1104 > 0.05
Mode	0.708 ± 0.661	1.021 ± 0.917	1.343 ± 1.041	0.1822 > 0.05	**0.0111 < 0.05**	**0.0243 < 0.05**
Median	0.379 ± 0.304	0.558 ± 0.576	1.028 ± 0.688	0.2005 > 0.05	**0.000639 < 0.05**	0.1469 > 0.05

Table 4 demonstrates that the healthy breast thermograms bear minute bilateral temperature difference, while there is a significant temperature difference between two breasts of benign and malignant breast thermograms. However, the bilateral temperature difference of a malignant breast thermogram is much higher than a benign breast thermogram.

By observing the p-value of significance test as demonstrated in Table 4, it is found that only the mean temperature is statistically significant in separating healthy thermograms from the benign ones, while all four temperature features are statistically significant in differentiating healthy thermograms from the malignant ones. However, except maximum and median temperature, the mean and mode temperatures are statistically significant in separating the benign thermograms from the malignant ones.

Since, we are dealing with different images of healthy, benign and malignant cases for temperature analysis, hence instead of directly comparing the temperature differences of a benign with the temperature differences of a malignant thermogram, we sort all the bilateral temperature difference values (obtained from each thermogram of any group) in ascending order for all four temperature features: mean, maximum, mode and median and then, plot them in same X-Y plan for comparison as illustrated in Fig. 3.

As depicted in Fig. 3(a), it has been seen that for almost all the malignant thermograms, the bilateral mean temperature differences are much higher than the bilateral mean temperature differences of benign and healthy thermograms. Similarly, the mean temperature differences in most of the benign cases are also higher than the mean temperature differences in healthy cases. Like mean, the bilateral maximum, mode and the median temperature differences of malignant thermograms (as shown in Fig. 3(b-d) respectively) are also much higher than the maximum, mode and median temperature differences in healthy and benign cases. However, unlike all malignant cases, for some benign and

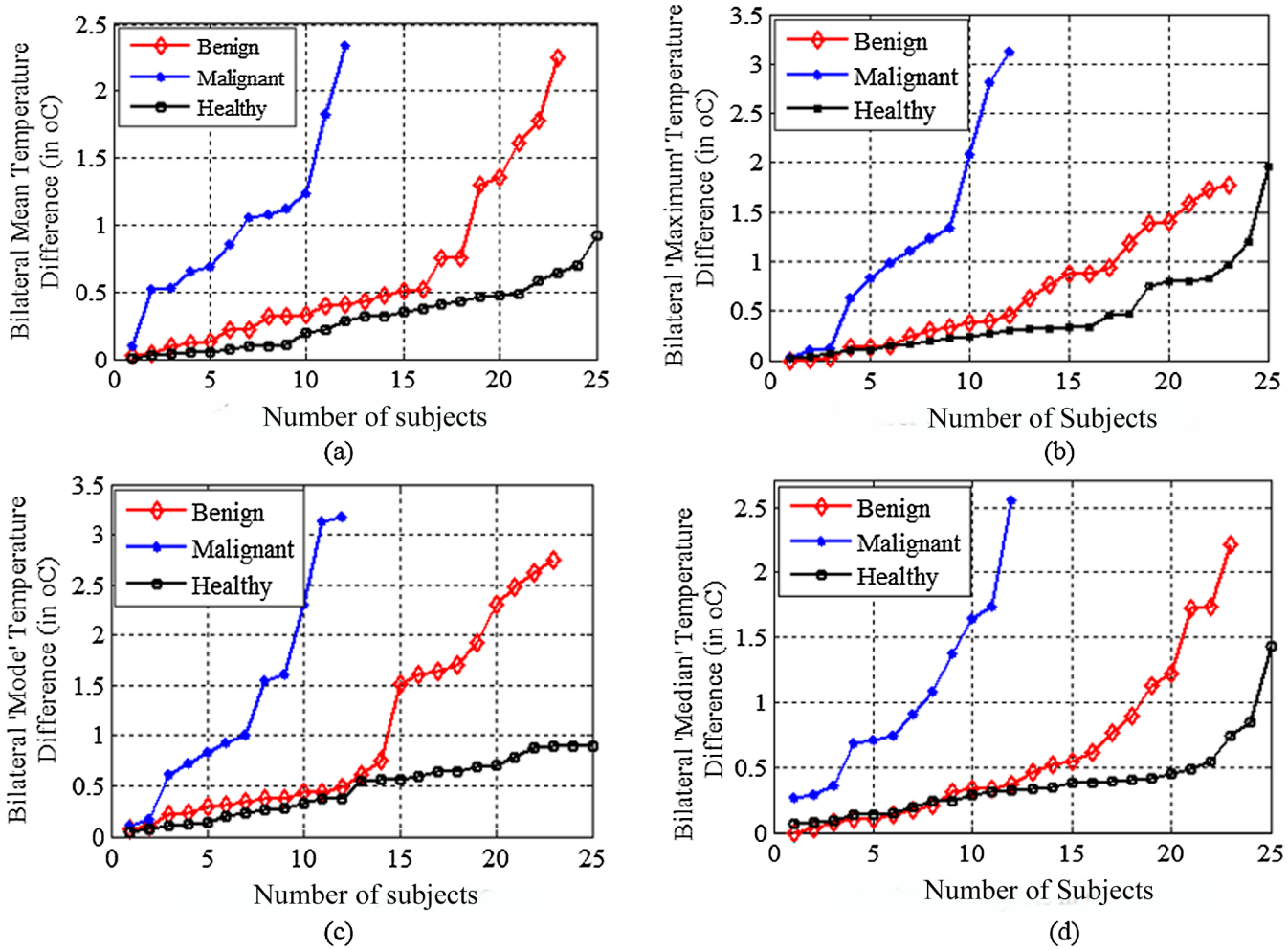

Fig. 3. (a) The bilateral mean temperature difference, (b) The bilateral maximum temperature difference, (c) The bilateral mode temperature difference and (d) The bilateral median temperature difference of each breast thermograms in healthy, benign and malignant groups.

healthy cases, the maximum and median temperature difference is almost similar, which may sometimes increase the false positive and false negative rate.

Thus, by separating the malignant cases from the healthy or benign cases, TBA of thermograms can identify the cases that need urgent medical attention. Hence, by pinpointing the suspicious cases through TBA, the IBT can provide more treatment options to the radiologists and also improves the survivability rate of the patients.

3.2. Intensity Based Analysis (IBA) of thermograms

The different temperature range of the breast surface temperature is represented with different pseudo colors in a breast thermogram. Hence, like the temperature analysis, the intensity value based analysis of the breast thermogram also plays an important role in early breast abnormality prediction. There are several color palettes with different pseudo colors to represent the breast thermograms. Here for the experimental purpose, among various color pallets, we have considered the "Rainbow HC" color pallet. The IBA has been performed in two ways: (a) Intensity Histogram Based Analysis and (b) Statistical Feature Based Analysis.

3.2.1. Intensity histogram based analysis

The "Rainbow HC" color pallet is an RGB image and for the IBA of thermograms, the intensity distributions of thermograms in each of R, G and B channel has been investigated. Along with the R, G, B histograms, the grayscale histogram of each breast thermogram is also analyzed for finding out the discriminability power of IBA in early breast abnormality detection. The R, G, B and grayscale histograms of the left and right breasts of a healthy, benign and malignant breast thermogram have been plotted in Fig. 4(a-c), (d-f) and (g-i) respectively.

As demonstrated in Fig. 4(a-b), in a healthy breast thermogram, the intensity distribution of left breast in all three R, G and B channels is almost similar to the intensity distribution of right breast in corresponding channels. Similarly, the grayscale distribution of left and right breast of a healthy breast thermogram as shown in Fig. 4(c) also illustrates the similarity of intensity distributions in both breasts. Moreover from Fig. 4(c), it can be concluded that in healthy breast thermograms, the dynamic range of left breast is almost similar to the dynamic range of the right breast. As illustrated in Fig. 4(d-e), considerable variations have been seen in the intensity distributions of the left and right breast of a benign breast thermogram in all three R, G and B channels. As shown in Fig. 4(d), in Red channel, the maximum number of pixels of left breast is found to acquire the intensity value in

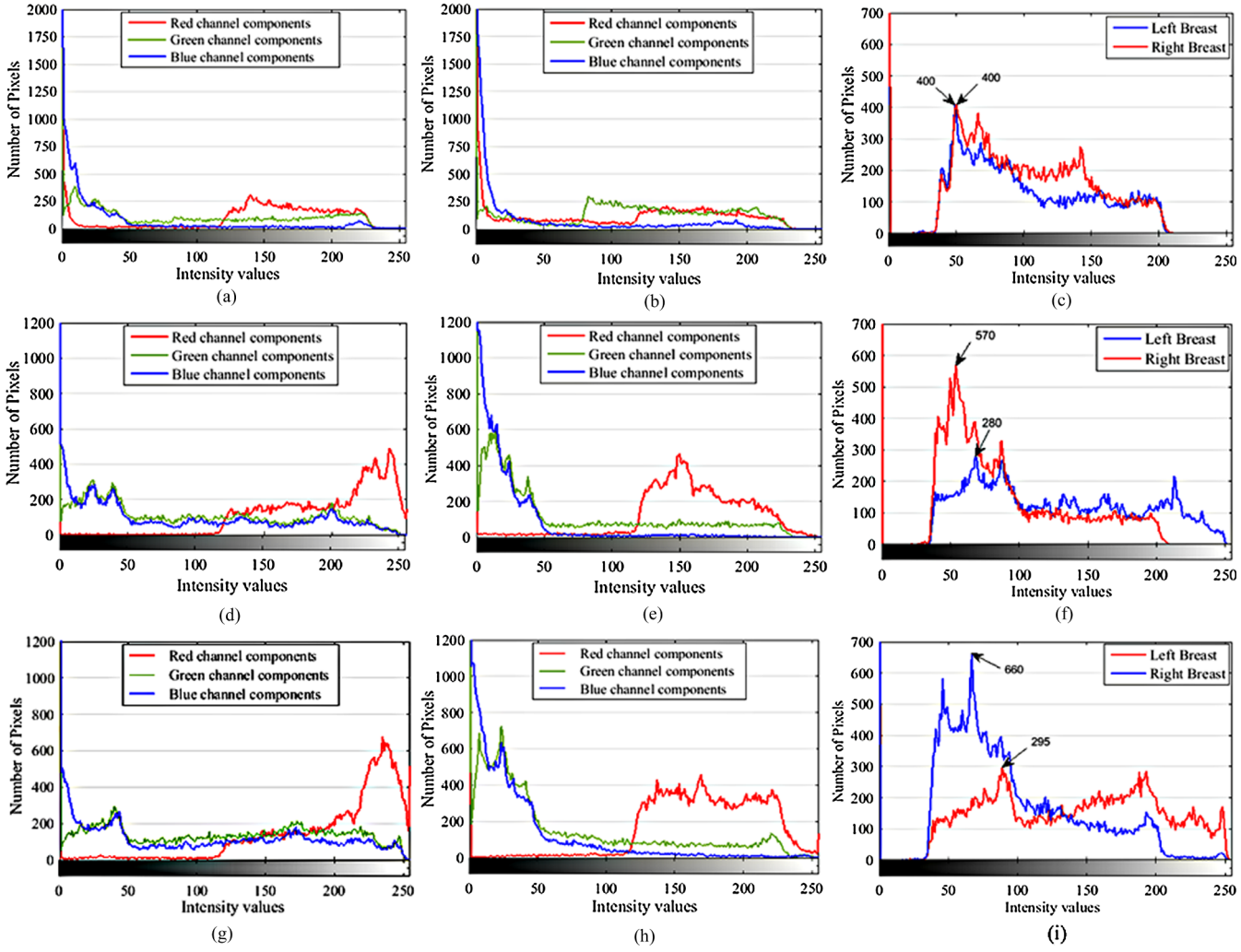

Fig. 4. The RGB histograms of (a) Left breast and (b) Right breast of a healthy thermogram; (c) The Gray level histogram of leftand right breast of a healthy thermogram; The RGB histograms of (d) Left breast and (e) Right breast of a benign breast thermogram; (f) The Gray level histogram of left and right breast of a benign breast thermogram; The RGB histograms of (g) Left breast and (h) Right breast of a malignant breast thermogram; (i) The Gray level histogram of left and right breast of a malignant breast thermogram.

the range of 220–250, while in the right breast, the maximum number of pixels acquire the intensity values in the range of 130–170. Moreover, Fig. 4(f) illustrates that the graylevel distribution of left breast is considerably different from the graylevel distribution of the right breast. A change in the dynamic range of left and right breast has also been seen in Fig. 4(f), where the dynamic range of the left breast is in between 30 and 200 and the dynamic range of the right breast is in between 0 and 250. Thus, from the RGB and graylevel intensity distribution, it is possible to separate the benign thermograms from the healthy one. Like benign, in malignant cases also, the intensity distribution of left breast is different from the intensity distribution of right breast in all R, G and B channels. As illustrated in Fig. 4(g), in red channel the highest number of pixels of left breast is found to acquire the intensity values in the range of 210–255, while in the right breast the maximum number of pixels acquires the intensity values in the range of 110–225. Similarly, compared to the green components in the left breast, the right breast has more green components. Besides, as demonstrated in Fig. 4(i), the graylevel distribution of left breast is vastly different from the graylevel distribution of the right breast and the dominant dynamic range of left breast is found to be 0–200, while the dynamic range of right breast is 30–250.

Thus, by analyzing the left and right breasts' intensity distributions of breast thermograms, it is possible to predict the presence of an abnormality in thermograms. Moreover, intensity analysis of breast thermograms also enables the categorization of breast thermograms into healthy, benign and malignant group.

3.2.2. Statistical feature based analysis

This section aims to represent the discriminability of intensity histograms in a quantitative way by computing the first order statistical (FOS) features which are also known as histogram based features. A set of six FOS features including mean, entropy, skewness, kurtosis, variance and standard deviation (std) has been extracted from the intensity histograms of each R, G, B channels and from the grayscale image. Computation of these features for both left and right breasts is followed by the calculation of the bilateral feature differences. The average of the bilateral feature differences of all breast thermograms of healthy, benign and malignant groups in each channel is listed in Table 5. Along with the average feature value differences, the statistical significance (p-value) of each feature has also been evaluated by using Wilcoxon non-parametric test to verify their efficiency in differentiating the malignant, benign and healthy thermograms. The p-values of each feature have been listed in Table 5. However, it is worth mentioning that the p-value of each feature mentioned in Table 5 is valid to only thermograms in "Rainbow HC"color pellet and the p-values may vary if thermograms in different color pellet are used. As demonstrated in Table 5, it has been seen that among all the features of red channel image, only r_mean is statistically significant ($p < 0.05$) in differentiating the healthy thermograms from benign and malignant thermograms, but it is not significant in differentiating the benign thermograms from the malignant ones.Similarly, among all the green channel image features, g_mean, g_skewness, g_variance and g_std are found to be statistically significant ($p < 0.05$) in differentiating malignant thermograms from the healthy and benign ones. But, these four features are not statistically significant to differentiate the healthy thermograms from the benign ones. Likewise among all blue channel features, only b_mean, b_variance and b_std can significantly differentiate the healthy thermograms from the benign and malignant ones. Moreover along with these three blue channel features, b_entropy can also separate the healthy thermograms from malignant ones. However unlike these three channel features, three grayscale image features mean, variance and std are found to be statistically significant ($p < 0.05$) in differentiating each category of thermograms. Unlike remaining features of the grayscale image, the entropy is also significant ($p < 0.05$) in differentiating healthy thermograms from benign and malignant ones.

Moreover to conclude the efficiency of extracted features in breast abnormality prediction, their sole and combined prediction performance should be evaluated by using a machine learning technique. Hence, feature extraction is followed by evaluating the prediction performance of these feature sets in classifying breast thermograms into healthy, benign and malignant groups. However for choosing the most efficient classifier for performance evaluation of feature sets, we rely on the findings of our previous works [21,22]. In [21], the performance of different classifiers: Support Vector Machine (SVM), K-Nearest

Table 5
Bilateral feature difference in each category of breast thermograms.

	Statistical Features	Healthy (H)	Benign (B)	Malignant (M)	p-val (H Vs. B)	p-val (H Vs. M)	p-val (B Vs. M)
Red Channel Features	r_mean	9.313 ± 9.28	16.57 ± 13.459	25.03 ± 19.103	**0.0184 < 0.05**	**0.0026 < 0.05**	0.1086 < 0.05
	r_entropy	0.114 ± 0.093	0.098 ± 0.059	0.129 ± 0.119	0.5403 > 0.05	0.4932 < 0.05	0.4506 > 0.05
	r_skewness	0.247 ± 0.219	0.265 ± 0.175	0.257 ± 0.312	0.2253 > 0.05	0.7902 < 0.05	0.7987 < 0.05
	r_kurtosis	0.645 ± 0.583	0.896 ± 0.628	0.932 ± 0.720	0.0892 > 0.05	0.1550 < 0.05	0.5635 > 0.05
	r_variance	0.009 ± 0.022	0.006 ± 0.011	0.017 ± 0.037	0.5669 > 0.05	0.0756 > 0.05	0.0548 > 0.05
	r_std	0.022 ± 0.010	0.017 ± 0.005	0.039 ± 0.018	0.4955 > 0.05	0.0616 > 0.05	0.0590 > 0.05
Green Channel Features	g_mean	13.39 ± 11.397	11.87 ± 7.497	27.52 ± 17.014	0.5492 > 0.05	**0.0046 < 0.05**	**0.0026 < 0.05**
	g_entropy	0.130 ± 0.158	0.149 ± 0.109	0.179 ± 0.1445	0.0856 > 0.05	0.0918 > 0.05	0.2787 > 0.05
	g_skewness	0.301 ± 0.264	0.246 ± 0.207	0.605 ± 0.363	0.7747 > 0.05	**0.0041 < 0.05**	**0.0009 < 0.05**
	g_kurtosis	0.419 ± 0.428	0.335 ± 0.285	0.529 ± 0.321	0.6530 > 0.05	0.1171 > 0.05	**0.0139 < 0.05**
	g_variance	0.011 ± 0.021	0.009 ± 0.011	0.018 ± 0.0165	0.4953 > 0.05	**0.0096 < 0.05**	**0.0007 < 0.05**
	g_std	0.022 ± 0.011	0.017 ± 0.006	0.034 ± 0.009	0.4776 > 0.05	**0.0187 < 0.05**	**0.0014 < 0.05**
Blue Channel Features	b_mean	8.333 ± 5.498	23.11 ± 17.717	26.85 ± 19.044	**0.0008 < 0.05**	**0.0006 < 0.05**	0.2553 > 0.05
	b_entropy	0.440 ± 0.382	0.716 ± 0.579	0.814 ± 0.439	0.0660 > 0.05	**0.0106 < 0.05**	0.2669 > 0.05
	b_skewness	0.828 ± 0.488	0.803 ± 0.774	0.798 ± 0.580	0.8476 > 0.05	0.6782 > 0.05	0.3157 > 0.05
	b_kurtosis	6.166 ± 5.343	4.008 ± 4.416	3.018 ± 2.249	0.9681 > 0.05	0.9539 > 0.05	0.4929 > 0.05
	b_variance	0.009 ± 0.019	0.026 ± 0.050	0.037 ± 0.045	**0.0020 < 0.05**	**0.0051 < 0.05**	0.0838 > 0.05
	b_std	0.029 ± 0.007	0.063 ± 0.021	0.079 ± 0.022	**0.0184 < 0.05**	**0.0007 < 0.05**	0.1227 > 0.05
Grayscale Image Features	mean	6.968 ± 6.786	11.66 ± 8.726	16.76 ± 16.76	**0.0184 < 0.05**	**0.0006 < 0.05**	**0.0435 < 0.05**
	entropy	0.088 ± 0.093	0.198 ± 0.127	0.241 ± 0.241	**0.0001 < 0.05**	**0.0001 < 0.05**	0.1817 > 0.05
	skewness	0.222 ± 0.211	0.24 ± 0.170	0.353 ± 0.260	0.2680 > 0.05	0.0574 > 0.05	0.1020 > 0.05
	kurtosis	0.252 ± 0.264	0.378 ± 0.318	0.444 ± 0.346	0.0554 > 0.05	0.0574 > 0.05	0.2669 > 0.05
	variance	0.004 ± 0.009	0.008 ± 0.016	0.015 ± 0.017	**0.0052 < 0.05**	**0.0000 < 0.05**	**0.0048 < 0.05**
	std	0.010 ± 0.004	0.021 ± 0.007	0.038 ± 0.007	**0.0089 < 0.05**	**0.0000 < 0.05**	**0.0043 < 0.05**

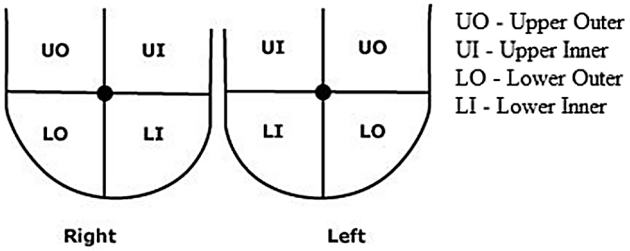

Fig 5. The four quadrants of Right and Left breast of a breast thermogram.

Table 6
Location of tumors in mammograms and in thermograms.

Locations of tumors	Patient Id with tumor	
	Mammograms	Thermograms
Upper (Left)	1, 3, **4**, 5, 6, 7, 9, 12, 15, 26, 27, 30,10, 13, 28	1, 3, 5, 6, 7, 9, 12, 15, 26, 27, 30,10, 13, 28
Upper (Right)	11, 14, 19, 23,10, 13, 28	11, 14, 19, 23,10, 13, 28
Lower (Left)	2,**8**	2
Lower (Right)	Nil	Nil
Periareolar (Left)	29	29
Periareolar (Right)	17	17

Neighborhood (KNN), Decision Tree (DT) and Artificial Neural Network (ANN) have been compared and among all, the SVM provides the highest classification accuracy. Similarly in [22], among seven different classifiers: SVM, ANN, KNN, DT, Random Forest, Linear Discriminant Analysis and AdaBoost, the SVM gives the best classification accuracy. Hence instead of using different classifiers, in this work the performance of the feature sets are evaluated by using only the SVM classifier. Thus by evaluating the efficiency of extracted feature set, it is possible to identify the most potential feature set.

3.3. Tumor Location Matching (TLM)

Besides quantitatively evaluating the potentiality of IBT to be used as a routine check-up tool in the asymptomatic population, it is necessary to correlate the suspicious region locations of abnormal thermograms with the tumor locations in mammograms or FNAC images. In medical practice, the tumor locations in a mammogram can be categorized into four quadrants: Upper outer quadrants (UOQ), Upper inner quadrants (UIQ), Lower outer quadrants (LOQ) and Lower inner quadrants (LIQ) as shown in Fig. 5. However since IBT is a functional imaging modality, the radiation emitted from a surface does not have a sharp boundary and can diffuse from one quadrant to other. Hence, categorization of the suspicious regions' locations of the thermograms in four quadrants may produce an erroneous conclusion, for which instead of categorizing the tumor locations into four quadrants, we have just categorized the suspicious areas as in upper half or in lower half of any breast. Table 6 demonstrates the matching of tumor locations in breast thermograms and corresponding mammograms or FNAC. The Patient Ids (as illustrated in Table 3), whose tumor locates either in upper or lower quadrant of mammograms and thermograms are listed in Table 6. Along with the upper and lower quadrants, the tumor locating near the Periareolar region of any breast are listed against the 'Periareolar' row of Table 6. However, while matching the tumor locations in mammograms and thermograms, it is worth to be noted that as illustrated in Table 3, for all abnormal cases, the location of tumors in mammograms is not present. Hence, for correlation we have considered only those Patient ids of Table 3 (1–15, 17, 19, 23, 26–30), whose mammographic tumor locations are available. Patient Ids of the subjects having tumors in both the breasts are listed in both left and right group of each location. As illustrated in Table 6, it has been seen that like mammography, IBT is also capable of pinpointing the tumor locations. But, in two cases with Patient Id 4 and 8, as presented in Table 6, IBT is incapable of showing the tumor location. However, with the capability of IBT in showing the exact location of tumor in 21 abnormal cases out of total 23 cases, the potential of IBT to be used as a routine check-up tool in asymptomatic patients has been proved.

4. Results

For evaluating the performance of TBA and IBA features in breast abnormality prediction, the extracted features are categorized into thirteen sets of features as follows-

(1) Red channel features (RF)
(2) Green channel features (GF)
(3) Blue channel features (BF)
(4) Grayscale image features (GrayF)
(5) Red channel features with $p < 0.05$ in any case (RSF)
(6) Green channel features with $p < 0.05$ in any case (GSF)
(7) Blue channel features with $p < 0.05$ in any case (BSF)
(8) Grayscale image features with $p < 0.05$ in any case (GraySF)
(9) Combination of all statistical features: RF, GF, BF & GrayF (RGBGrayF)
(10) Combination of all statistical features with $p < 0.05$: RSF, GSF, BSF &GraySF (RGBGraySF))
(11) Combination of all temperature features with $p < 0.05$ in any case (STemp)
(12) Mean temperature (MeanTemp)
(13) Combination of MeanTemp with RGBGraySF (SSigTempInt)

Categorization of TBA and IBA features into thirteen different feature sets is followed by the evaluation of the classification performance of each of these feature sets. The support vector machine (SVM) with radial basis function (RBF) kernel has been used for classification of thermograms. For evaluating the classification performance of each feature set, three well known and widely used evaluation metrics: accuracy, sensitivity and specificity have been used. The classification performance of each of these feature sets has been listed in Table 7.

Based on the classification performance of each of these thirteen feature sets, it has been seen that among all single channel feature sets (RF, GF, BF, GrayF, RSF, GSF, BSF and GraySF), the BF provides the highest prediction accuracy of 77.78% with sensitivity of 64.65% and specificity of 66.16%. However, in comparison to BF, the GSF feature set provides better sensitivity and specificity of 73.23% and 71.72% respectively with the classification accuracy of 76.39%. Moreover, in comparison to these single channel feature sets, the RGBGraySF containing the statistically significant features of all channels provides

Table 7
Classification accuracies of each feature set.

Feature sets	Prediction performance		
	Accuracy	Sensitivity	Specificity
RF	64.17	60.10	51.01
GF	74.17	78.79	63.13
BF	77.78	64.65	66.16
GrayF	74.44	63.13	68.69
RSF	63.50	46.97	66.16
GSF	76.39	73.23	71.72
BSF	68.06	45.96	73.74
GraySF	71.67	52.02	69.70
RGBGrayF	71.50	44.44	41.41
RGBGraySF	82.22	78.79	71.72
STemp	65.33	57.07	43.94
MeanTemp	70.89	62.63	52.53
SSigTempInt	**83.22**	**85.56**	**73.23**

much better classification accuracy of 82.22% with 78.79% sensitivity and 71.72% specificity.

Like the intensity features, while evaluating the classification performance of the temperature feature sets, it has been seen that the STemp feature set that comprises of the statistically significant temperature features provides a poor classification accuracy of 65.33%. Moreover, the classification performance of MeanTemp feature set is also not efficient enough to be used solely. However, the SSigTempInt feature set comprising of MeanTemp feature with the RGBGraySF feature set provides the highest classification accuracy of 83.22% with sensitivity 85.56% and specificity 73.23%. Thus, it can be concluded that consideration and combination of the statistically significant intensity and temperature features is crucial enough to validate the potentiality of IBT in breast abnormality detection.

5. Discussion

In spite of good advancements for diagnosis and treatment, cancer is still a big threat to our society. Among all cancers, the breast cancer is one of the leading causes of death among women worldwide and it becomes a significant public health concern. In India, due to the lack of medical facilities and poor breast cancer awareness, the breast cancer mortality rate is very high. Moreover, over the last few decades in India, the average age of developing breast cancer has shifted to 30–40 years. But, the restrictions of the gold standard method X-ray mammography to be used for screening in young women below 40 years of age demands the development of a safe and effective technology for screening of breast abnormality in young women.

Owing to this requirement of a breast screening modality that is capable enough to detect the breast abnormality before developing into a cancerous mass, this study evaluates the potentiality of IBT to be used as a routine check-up tool in asymptomatic population for early abnormality detection. Moreover, due to its non-invasiveness, radiation-free nature, it is applicable for women of all ages including nursing and pregnant women. For evaluating the potentiality of IBT, a thorough analysis of breast thermograms has been made in this study. Before performing the analysis of breast thermograms, the findings of IBT are validated with the clinical findings and with the findings of X-ray mammography and FNAC (if available) reports. Based on the findings of X-ray mammography/FNAC, the breast thermograms of the experimental dataset are categorized into three distinct classes: Healthy, Benign and Malignant. The temperature based and intensity based analysis of breast thermograms of each category concludes that the temperature and intensity distribution of left breast of a healthy thermogram is almost similar to the intensity distribution of the right breast. But, in case of benign and malignant breast thermograms, the intensity or temperature distribution of left breast noticeably varies from the intensity distribution of right breast. Moreover, with the highest classification accuracy of 83.22%, IBT can be used for early breast abnormality detection. Besides, by correlating the tumor location in thermograms and in mammograms or FNAC, it has been proved that the IBT is potential enough to be used as a routine check-up tool in asymptomatic patients and thus, can reduce the breast cancer incidence and mortality rate.

Although this study shows the efficiency of IBT to be used as a routine check-up tool, one limitation of this study is the small experimental dataset which we try to address in our future work. Moreover, the future studies will also deal with a dataset of asymptomatic patients to validate the findings of this study.

6. Conclusion

In this work, we have investigated the potentiality of IBT to be used as a screening tool in asymptomatic patients with the objective of detecting a breast disease before the onset of cancer. We perform a multistage evaluation of IBT to prove the efficiency of IBT. From the findings of the study, we now believe that IBT is potential enough to reach the masses rather waiting for masses to reach the tertiary centers for screening. Moreover, utilization of IBT in early breast cancer screening will improve the quality of healthcare systems in India by providing more treatment options to the patients and thus, reducing the mortality rate of breast cancer.

7. Conflict of interest

All authors declare that they don't have any conflict of interest.

8. Human subjects protections

This work is done by maintaining the ethical standards of AGMC with IRB approval number F.4 (5–2)/ AGMC/ Academic/ Project/ Research/2007/Sub-I/ 8199-8201.

Acknowledgment

The work presented here is being conducted in the Bio-Medical Infrared Image Processing Laboratory (BMIRD) of Computer Science and Engineering Department, Tripura University (A Central University), Suryamaninagar-799022, Tripura (W). The first author is grateful to Department of Science and Technology (DST), Government of India for providing her Junior Research Fellowship (JRF) under DST INSPIRE fellowship program (No. IF150970).

Funding

This work was supported by Department of Biotechnology (DBT), Govt. of India (Grant No. BT/533/NE/TBP/2013, Dated 03/03/2014).

References

[1] American Cancer Society: Cancer facts and Figures. Available at: www.cancer.org/docroot/STT/stt_0.asp.
[2] E.Y.K. Ng, N.M. Sudarshan, Numerical computation as a tool to aid thermographic Interpretation, J. Med. Eng. Technol. 25 (2001) 53–60.
[3] A. Berrington de González, G. Reeves, Mammographic screening before age 50 years in the UK: comparison of the radiation risks with the mortality benefits, Br. J. Cancer 93 (2005) 590–596.
[4] D. Kennedy, T. Lee, D. Seely, A comparative review of thermography as a breast screening technique, Integrative Cancer Therapies 8 (1) (2009) 9–16.
[5] J. Law, K. Faulkner, K.C. Young, Risk factors for induction ofbreast cancer by x-rays and their implications for breast screening, Br. J. Radiol. 80 (2007) 261–266.
[6] National Cancer Institute: SEER Stat Fact Sheets: Breasts. Available at: www.seer.cancer.gov/statfacts/html/ breast.html.
[7] E.Y.K. Ng, A review of thermography as promising noninvasive detection modality for breast tumour, Int. J. Therm. Sci. 48 (5) (2009) 849–859.
[8] N. Diakides, J.D. Bronzino, Medical infrared imaging, Taylor & Francis. New York, CRC, 2007.
[9] E.Y.K. Ng, E. Kee, Advanced integrated technique in breast cancer thermography, J. Med. Eng. Technol. 32 (2) (2008) 103–114.
[10] N. Golestani, M. EtehadTavakol, E.Y.K. Ng, Level set method for segmentation of infrared breast thermograms, EXCLI journal 13 (2014) 241–251.
[11] J. Koay, C. Herry, M. Frize, Analysis of breast thermography with an artificial neural network, in: Proc. 26th Annual IEEE International Conference on Engineering in Medicine and Biology Society (IEMBS), 2004, pp. 1159-1162; San Francisco, CA, USA.
[12] J.R. Keyserlingk, P.D. Ahlgren, E. Yu, N. Belliveau, Infrared imaging of breast: Initial reappraisal using high-resolution digital technology in 100 successive cases of stage I and II breast cancer, Breast J. 4 (4) (1998) 245–251.
[13] B.B. Lahiri, S. Bagavathiappan, T. Jayakumar, J. Philip, Medical applications of infrared thermography: a review, Infrared Phys. Technol. 55 (4) (2012) 221–235.
[14] P. Gamagami, Atlas of mammography: new early signs in breast cancer, Blackwell Science (1996).
[15] T. Sarigoz, T. Ertan, O. Topuz, Y. Sevim, Y. Cihan, Role of digital infrared thermal imaging in the diagnosis of breast mass: a pilot study: diagnosis of breast mass by thermography, Infrared Phys. Technol. 91 (2018) 214–219.
[16] J.W.K. Louis, M. Gautherie, Long term assessment of breast cancer risk by thermal imaging, Biomed Thermology 279–301 (1982).
[17] E.Y.K. Ng, S.C. Fork, A framework for early discovery of breast tumor using thermography with artificial neural network, Breast J. 9 (4) (2003) 341–343.
[18] E.F.J. Ring, K. Ammer, The technique of infrared imaging in medicine, Thermol. Int. 10 (1) (2000) 7–14.

[19] M.K. Bhowmik, U.R. Gogoi, G. Majumdar, D. Bhattacharjee, D. Datta, A.K. Ghosh, Designing of ground truth annotated DBT-TU-JU breast thermogram database towards early abnormality prediction, IEEE J. Biomed. Health Informatics (J-BHI) 22 (4) (2017) 1238–1249.
[20] M.K. Bhowmik, U.R. Gogoi, K. Das, A.K. Ghosh, D. Bhattacharjee, Majumdar G: Standardization of infrared breast thermogram acquisition protocols and abnormality analysis of breast thermograms", in Proc. SPIE Commercial + Scientific Sensing and Imaging, pp. 986115-(1-18), 2016.
[21] U.R. Gogoi, M.K. Bhowmik, A.K. Ghosh, D. Bhattacharjee, G. Majumdar, Discriminative Feature Selection for Breast Abnormality Detection and Accurate classification of Thermograms, in: Proc. IEEE International Conference on Innovations in Electronics, Signal Processing and Communication (IESC), pp. 39-44, 2017.
[22] U.R. Gogoi, M.K. Bhowmik, D. Bhattacharjee, A.K. Ghosh, Singular value based characterization and analysis of thermal patches for early breast abnormality detection, Australasian Phys. Eng. Sci. Med. 41 (4) (2018) 861–879.
[23] J.H. Tan, E.Y.K. Ng, U.R. Acharya, C. Chee, Infrared thermography on ocular surface temperature: a review, Infrared Phys. Technol. 52 (2009) 97–108.
[24] B.F. Jones, A reappraisal of the use of infrared thermal image analysis in medicine, IEEE Trans. Med. Imaging 17 (1998) 1019–1027.
[25] J.D. Hardy, The radiation of heat from the human body (I–IV). Journal of Clinical Investigation 13:593–620 & 817–883, 1934.
[26] J.D. Hardy, C. Muschenheim, The radiation of heat from the human body (V), J. Clinical Investigation 15 (1936) 1–8.
[27] R.B. Barnes, Thermography of the Human body, Science 140 (1963) 870–877.
[28] S.V. Francis, M. Sasikala, S. Saranya, Detection of breast abnormality from thermograms using curvelet transform based feature extraction, J. Med. Syst. 38 (4) (2014) 1–9.
[29] E.Y.K. Ng, L.N. Ung, F.C. Ng, L.S.J. Sim, Statistical analysis of healthy malignant breast thermography, Int. J. Med Eng. Technol. 25 (6) (2001) 253–263.